


Article

Comprehensive Learning Particle Swarm Optimized Fuzzy Petri Net for Motor-Bearing Fault Diagnosis

Chuannuo Xu, Jiming Li and Xuezhen Cheng * 

College of Electrical Engineering and Automation, Shandong University of Science and Technology,
Qingdao 266590, China

* Correspondence: chengxuezhen@sdust.edu.cn; Tel.: +86-135-0532-4619

Abstract: Petri net is a widely used fault-diagnosis algorithm. However, it presents poor fault-diagnosis effectiveness and accuracy caused by the parameter setting and adjustment, depending entirely on expert experience in a system with a single input signal type. To address this problem, a comprehensive learning particle swarm optimized fuzzy Petri net (CLPSO-FPN) algorithm is proposed for motor-bearing fault diagnosis. CLPSO is employed to obtain an adaptive system parameter set to reduce the fault-diagnosis error caused by human subjective factors. Moreover, a new proposed concept of the transition influence factor replaces the traditional transition confidence to improve the nonlinear expression ability of traditional Petri nets, which suppresses the space explosion problem of the fault-diagnosis model. Finally, experiments are implemented on a dataset of motor bearings. Compared with traditional faults diagnosis methods, the proposed method realized better performance in the fault location and prediction functions of motor bearings, which is beneficial for troubleshooting and motor maintenance.

Keywords: comprehensive learning particle swarm optimization; fuzzy Petri Net; motor fault diagnosis; vibration signal; transition influence factor



Citation: Xu, C.; Li, J.; Cheng, X.
Comprehensive Learning Particle
Swarm Optimized Fuzzy Petri Net
for Motor-Bearing Fault Diagnosis.
Machines **2022**, *10*, 1022. <https://doi.org/10.3390/machines10111022>

Academic Editors: Benben Jiang,
Qiugang Lu and Yang Liu

Received: 24 September 2022

Accepted: 2 November 2022

Published: 3 November 2022

Publisher's Note: MDPI stays neutral with regard to jurisdictional claims in published maps and institutional affiliations.



Copyright: © 2022 by the authors. Licensee MDPI, Basel, Switzerland. This article is an open access article distributed under the terms and conditions of the Creative Commons Attribution (CC BY) license (<https://creativecommons.org/licenses/by/4.0/>).

1. Introduction

Many faults are caused by abrasion, high load and other complex working environments of motor bearings, and seriously affect the safe and stable operation of the motor [1]. Moreover, nonlinear and fuzzy fault relations of each functional module of the motor are averse to equipment fault diagnosis and elimination [2–4]. Therefore, real time and accurate fault-diagnosis methods for motor bearings represent a trending research topic [5–7].

At present, motor-bearing fault-diagnosis methods mainly include quantitative and qualitative methods, among which the data-driven method based on quantitative analysis is very common. Deng et al. proposed a method based on wavelet transform, fuzzy entropy and a support vector machine [8], which could effectively remove interference signals and improve the fault-diagnosis ability under strong noise. However, the frequency spectrum could not be divided adaptively, and the fault diagnosis lacked adaptability. Xu et al. proposed a fault-diagnosis method based on empirical mode decomposition (EMD) and principal component analysis (PCA) [9]. The main fault signals were extracted by EMD, and the dimensions of feature vectors were reduced by a PCA to achieve an effective reduction in fault feature information. Li et al. proposed a fault-diagnosis method based on a least square support vector machine [10], which combined the information fusion of nonlinear features and time-domain features to address the problem of low fault classification accuracy. Xiao et al. proposed a data enhancement method based on 2D greyscale images and an auxiliary classification generation antagonistic network [11]. The method could effectively reduce the number of training parameters of the deep learning network and improve the accuracy of fault identification, as well as the speed of network training. The above quantitative analysis was based on collecting the failure data of signal

analysis by extracting feature information to realize fault location. However, in a complex motor fault relation between each function module in the system with nonlinear and fuzzy features, some function modules from the cause of the problem cannot be diagnosed by means of data-driven methods and lack integrity.

The graph theory method based on qualitative analysis can establish the system model diagram according to the internal knowledge of the system, reflecting the logical relationship between the system modules. Thus, it is widely used in the field of system fault diagnosis. Among such methods, Petri net is one of the most commonly used. Zhu et al. proposed an efficient diagnosis algorithm based on labeled Petri nets, which is more efficient in comparison with the existing integer linear programming (ILP)-based approaches [12]. Zhang et al. carried out rigorous mathematical reasoning on fuzzy Petri nets and the reasoning process of the matrix [13] established a solid theoretical foundation for the development of fuzzy Petri nets applications. Arichi et al. proposed an approach based on two main steps: (i) designing an algebraic observer for estimating the markings and the transitions of a partially observed Petri nets; (ii) presenting algorithms to detect and identify faults, based on a comparison of the estimation of both the transitions and markings of the faulty system provided by an algebraic observer with those of the normal system [14]. Wang et al. proposed the particle swarm optimization (PSO) algorithm to optimize the fault diagnosis of Petri nets [15], but the traditional PSO algorithm for multidimensional parameter optimization achieved premature convergence and poor local optimization ability. The above qualitative analysis method based on a Petri net can realize fault prediction and positioning functions by deductive reasoning according to the logical relationship between each module of the system, which improves the integrity of fault diagnosis. However, the traditional fault-diagnosis method based on Petri nets can only handle discrete fault signals, and fault diagnosis lacks timeliness. To address the above problems, a continuous Petri net with maximum velocity variation was proposed [16,17]. Based on the traditional Petri net, the concept of dynamic time identification and transition excitation velocity was introduced in this method. Additionally, continuous signals were discretized through system parameters with time characteristics to realize the purpose of processing continuous signals. This set the theoretical foundation of the Petri net in the continuous signal processing field. Based on the characteristics of continuous Petri nets and discrete Petri nets, a hybrid Petri net dynamic modeling approach was proposed and applied to the fields of machinery manufacturing, transportation and robot control [18,19]. This method could process the continuous signal and the discrete signal independently, realize the information exchange between the two systems through the conversion of the continuous-discrete controller and the discontinuous-continuous controller and achieve dynamic analysis ability. Alejandro Bustos et al. [20,21] proposed a method that relied on classical signal processing techniques to identify the vibration analysis and operation status of railway bogies, and later proposed a mechanical condition monitoring method based on vibration analysis that supported two new signal processing techniques. However, the above diagnosis method based on Petri net relied on expert experience in its algorithm and in the parameter setting of the model, which was susceptible to human subjective factors and lacked objectivity.

Aiming at the problems of the traditional Petri net fault-diagnosis method with a single input signal and the lack of integrity and timeliness of the traditional motor-bearing fault-diagnosis method, according to an offline and an online algorithm [22], a fault-diagnosis method of motor bearing based on CLPSO-FPN is proposed: the EMD method is used to obtain discrete fault classification signals to activate the discrete signal processing system, which addresses the problems of the lack of integrity of traditional quantitative analysis methods in fault diagnosis and the lack of timeliness of qualitative analysis methods in fault diagnosis. The concept of transition influence factor is defined, and a comprehensive learning particle swarm optimization algorithm is proposed to optimize the parameters of the fault-diagnosis model, improve the adaptability of the fault-diagnosis model, reduce the influence of human subjective factors on the fault-diagnosis results, improve the accuracy

of fault identification and suppress the space explosion of the fault-diagnosis model of complex systems.

The main innovations are as follows: (1) the concept of transition influence factor is proposed to replace the traditional transition credibility, improve the nonlinear expression ability of traditional Petri nets and suppress the problem of space explosion in diagnostic models. (2) The comprehensive learning particle swarm optimized fuzzy Petri net algorithm is applied to supervise and train the fault-diagnosis model to obtain an adaptive system parameter set, which solves the problem pertaining to the setting and adjustment of parameters in traditional fault-diagnosis methods relying entirely on expert experience and the problem of the parameter setting lacking regularity, and reduces the fault-diagnosis error caused by human subjective factors.

2. Fault-Diagnosis Model Architecture Based on CLPSO-FPN

As a system modeling tool, Petri net has superior performance in discrete event processing. However, the system state usually includes two kinds of continuous and discrete cases, making it difficult to realize the dynamic analysis of the system by only relying on the discrete event processing mechanism of a Petri net. To improve the continuous signal processing ability of Petri nets, the CLPSO-FPN fault-diagnosis method was proposed in this paper, and its architecture is shown in Figure 1.

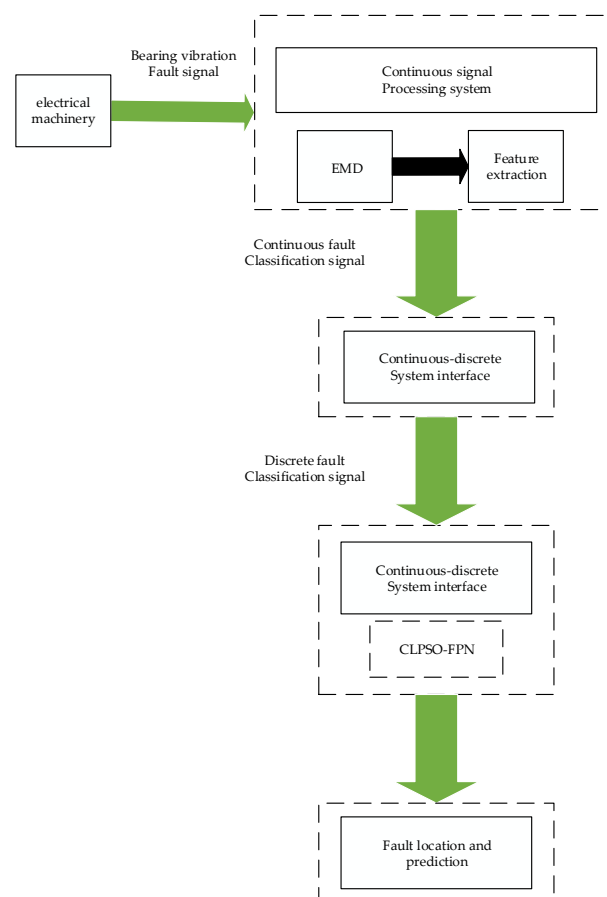


Figure 1. The structure diagram for fault-diagnosis system of CLPSO-FPN.

The continuous signal processing system in Figure 1 applied continuous signal processing technology to classify the real-time bearing-fault signals collected by the sensor and transmitted the obtained discrete fault classification signals to the discrete signal processing system to activate the discrete signal processing system. The discrete signal processing system optimized the traditional transition based on the transition influence

factors, constructed the fault-diagnosis model of CLPSO-FPN, obtained the probability of fault occurrence of fault events of relevant modules through forward reasoning and reverse reasoning and realized the accurate diagnosis of motor-bearing faults.

3. Continuous Fault Signal Processing Based on EMD

A continuous signal processing system can complete the processing and classification of continuous fault signals, which is the premise of fault location and prediction of fault-diagnosis systems. To ensure the normal operation of the fault-diagnosis system, EMD was applied in this paper to realize the effective processing of continuous fault signals. The processing system flow is shown in Figure 2.

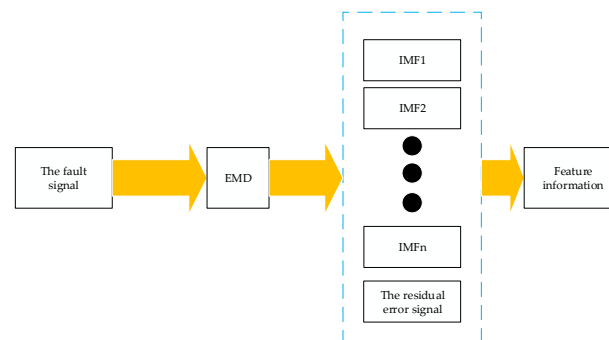


Figure 2. The flow of continuous fault data processing.

After the fault signal was processed by EMD, the IMF components were generated and the characteristic information was obtained.

The original data [23] were obtained from the fault data collected by the SKF6205 bearing drive end acceleration sensor in the laboratory of Case Western Reserve University in the United States. The fault signal is shown in Figure 3.

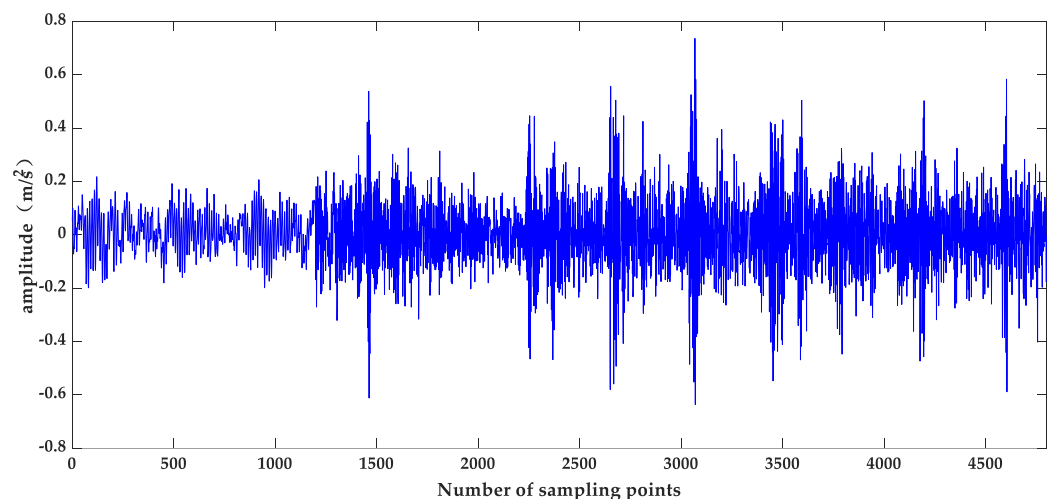


Figure 3. The signal of bearing fault.

EMD is an effective way to deal with nonlinear and nonstationary signals with a high time frequency resolution, which can decompose fault signals according to the frequency of the signals and obtain a series of intrinsic mode functions (IMFs) with the main fault information. Compared with the problem of the short-time Fourier transform (STFT) and wavelet transform being limited to the selection of window function and wavelet basis function, EMD has the characteristics of adaptive decomposition, which enables it to process continuous fault signals collected in real time and gives it a high degree of applicability.

A large amount of fault information is contained in high-frequency fault signals. Because empirical mode decomposition technology can obtain IMF at different frequencies, it is convenient to screen out high-frequency fault signals for feature extraction and signal processing.

On the basis of the literature [24–27], this paper used EMD to process continuous fault signals and selected IMF fault signals in the high-frequency band for fault feature processing. The first five IMF components are shown in Figure 4. It can be seen from Figure 4 that the first four IMF components had obvious characteristics, so the first four IMF components were selected in this paper [28,29].

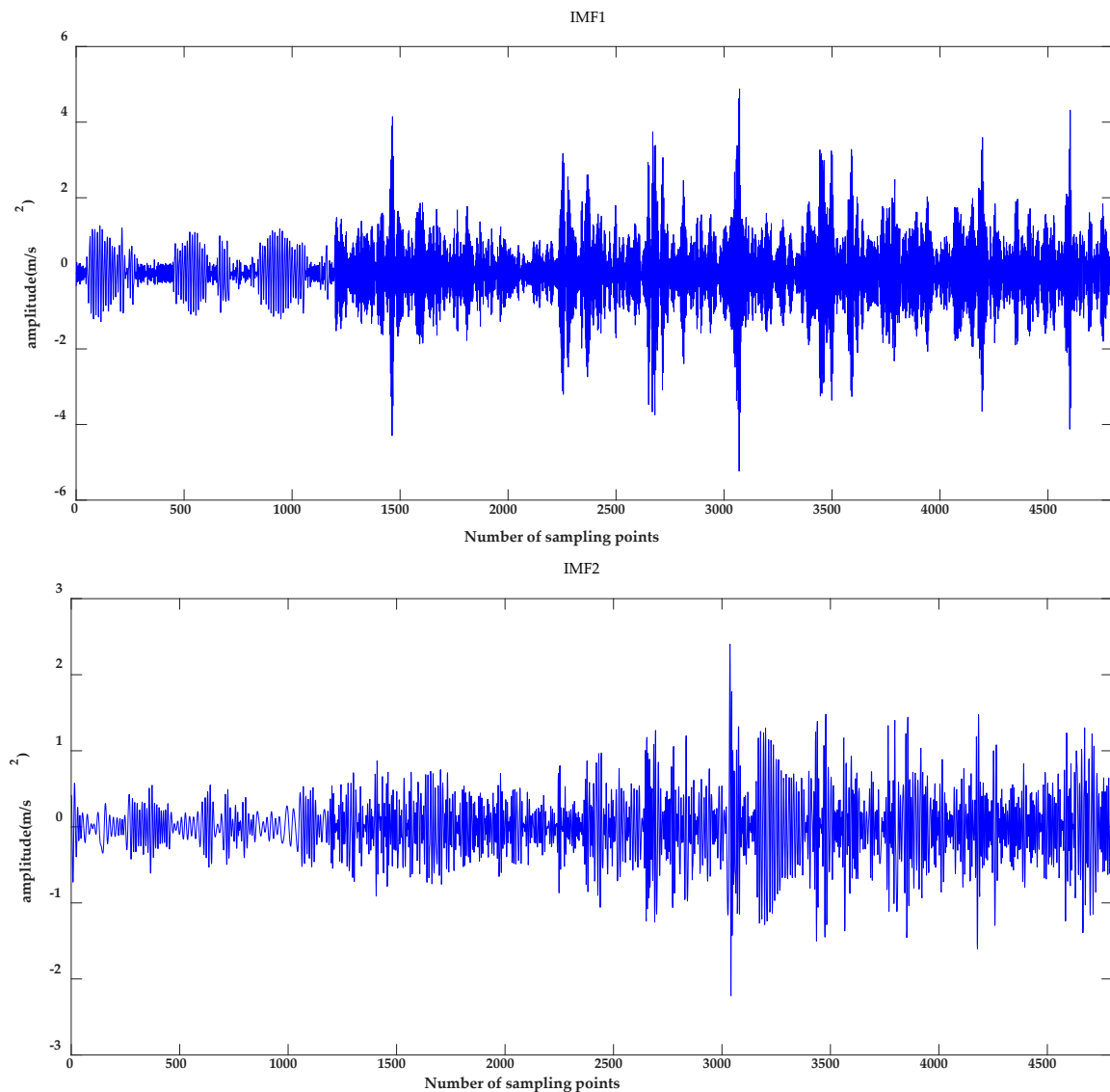


Figure 4. Cont.

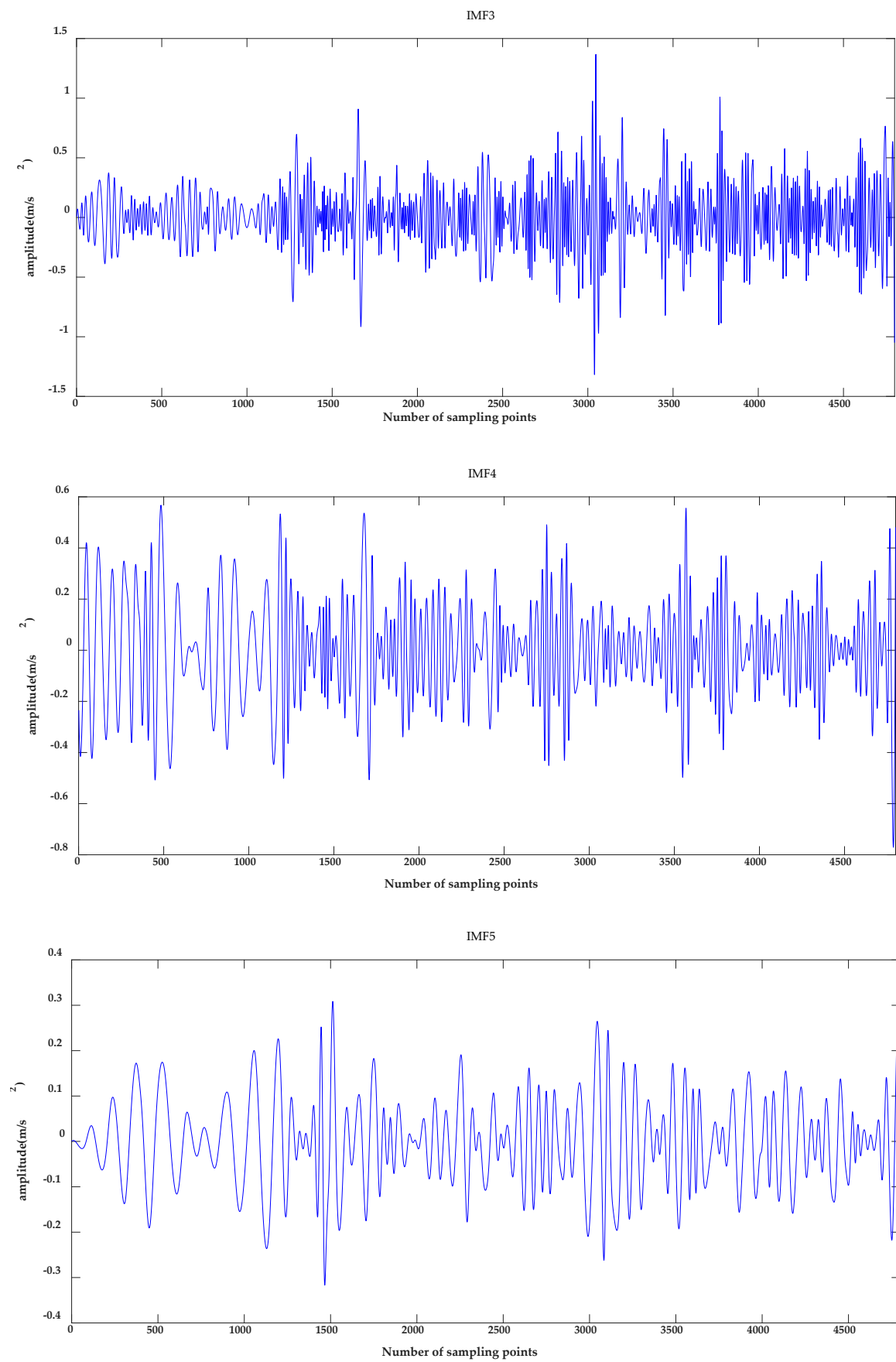


Figure 4. The results of EMD decomposition.

Conversion of Fault Classification Information

To ensure the accurate activation of the fault-diagnosis model of the discrete signal processing system, it is necessary to further transform the fault signals and screen out the invalid labels. Its processing flow is shown in Figure 5.

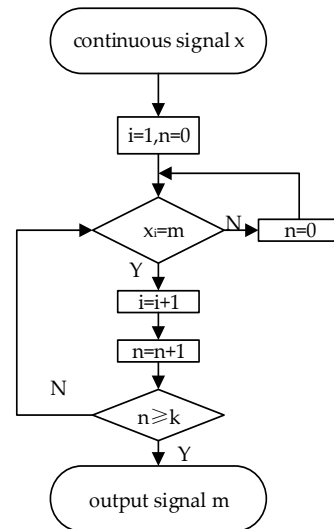


Figure 5. The flow of fault information conversion.

In Figure 5, x is the fault signal label, m is the label value of failure, n is the number of m tags appearing continuously and k is the output threshold of the label. When the number of tags that continuously appear in the tag is not less than the k value, it is confirmed that the fault represented by the m tag has occurred, and the m tag is output to the discrete signal processing system to realize the activation of the corresponding fault library.

4. The Fault-Diagnosis Method Based on CLPSO-FPN

A discrete signal processing system is a functional system for fault location and prediction, which mainly includes discrete fault data processing, fault-diagnosis model optimization and fault-diagnosis reasoning.

4.1. Discrete Fault Data Processing

Discrete fault data processing is the key to fault location and prediction. Based on the modeling method of CLPSO-FPN, accurate fault model construction was realized according to the discrete information obtained by processing. By dealing with the system structure and fault logic, the system fault location, fault type classification and fault cause analysis were realized, and the establishment of a fault event table was completed to provide the basis for the establishment of the system fault-diagnosis model.

Aiming at discrete fault data of complex motor systems, combining expert experience and engineering practice, this paper adopted the fuzzy theory. Fuzzy processing on the fault occurrence probability of each module was obtained by statistics and was used for determining the correlation between the confidence degree of the database and the fault occurrence probability [30], as shown in Table 1.

Table 1. The fuzzy definition of place value.

Possibility of Failure	Probability of Failure	Library Confidence
Inevitable	(50–100%)	[0.96, 1.00]
Easily happened	(40–50%)	[0.81, 0.95]
Occurs more easily	(30–40%)	[0.76, 0.80]
May occur	(10–30%)	[0.51, 0.75]
Not likely to happen	(0–10%)	[0.35, 0.50]

If information contains a significant amount of uncertainty during reasoning analysis, it is necessary to generate statistics on the occurrence probability of various faults. This reasoning analysis is called probabilistic reasoning. The problem of applying the Bayes method to reasoning is conditional probability reasoning. When drawing a conclusion, one should refer to the sample information observed at that time, and also to relevant past experience and common sense. To address the problem of fewer or uncertain fault data for some fault modules, the Bayesian method [31] was adopted to increase the confidence of the fault module library. This method effectively realized the accurate conversion of knowledge and experience to rules, and was conducive to solving the problem of empirical assignment.

Employing the "Reliability data of non-electronic parts 3" as discrete fault data, the fault event table in Table 2 and the statistical table of fault event confidence in Table 3 were obtained through discrete data processing. The confidence vector of the base failure p_1 to p_{11} was calculated as follows: $\alpha = (0.658, 0.750, 0.785, 0.810, 0.875, 0.756, 0.850, 0.775, 0.880, 0.710, 0.650)$.

Table 2. The table of bearing fault event.

Libraries	Failure Events	Libraries	Failure Events
p_1	motor is mixed with impurities	p_{11}	load overload
p_2	aging of rotor winding	p_{12}	low resistance of rotor winding
p_3	Inter-turn short circuit of rotor	p_{13}	short circuit of rotor winding
p_4	interphase rotor short circuit	p_{14}	bearing wear
p_5	scanning cage malfunction	p_{15}	fatigue peeling of bearing
p_6	rolling body fault	p_{16}	abnormal motor vibration
p_7	outer ring fault	p_{17}	bearing fracture
p_8	inner ring fault	p_{18}	rotor current increases
p_9	sweep the chamber	p_{19}	bearing temperature rise
p_{10}	the rotor broken bar	p_{20}	bearing fault

Table 3. The table of failure event place value.

Serial Number	The Cause of the Problem	The Fault Phenomenon	Library Confidence
1	p_1, p_2, p_3, p_4	p_{20}	0.144
2	p_5, p_6, p_7	p_{20}	0.658
3	p_7, p_8	p_{20}	0.790
4	p_9, p_{10}, p_{11}	p_{20}	0.769

4.2. Fault-Diagnosis Model Optimization Based on CLPSO-FPN

Petri net is a mathematical representation of discrete and parallel systems. Its graphical expression is a network information flow model, which is mainly used for dynamic modeling of discrete events. It is composed of repositories, tokens, transitions and directed arcs. The library is used to describe the status or premise of system events. The token represents the dynamic information of Petri nets, which exists in the library. The number of tokens represents the number of dynamic information resources stored in the library. Transitions represent events used to change the state of Petri nets. A directed arc connects two different depots through transitions, indicating the relationship between the two depots. When the transition triggers the ignition and causes the change of the token of the depot, the token will flow to the next depot along the direction of the directional arc. Each directional arc has a weight, which is called the arc weight. The occurrence of transition events is called transition ignition, and then token flows to the next level of the library according to the direction of the directed arc. Therefore, with the change of time, the token distribution of the Petri net changes, which illustrates the dynamics of the Petri net. This distribution of tokens in the repository is called repository identification. The state transition of the Petri net model is local, which is only related to the extension of events. It only involves a transition connecting the state change of the library through the input and output arcs,

which is a key characteristic of the Petri net. When a token appears in a library, the events represented by the library occur, and vice versa.

Petri nets use graphical language to describe the relationship between the library and the change. In the graphical language, the library is represented by “○”; the transition is represented by “■”; the token is represented by a small black dot “●”; and the directed relationship between the transition and the repository is represented by “∩”. At this time, the input matrix I reflects the connection matrix from the depot to the transition, and the output matrix O reflects the connection matrix from the transition to the depot.

To improve the nonlinear expression ability of the traditional Petri net and suppress the spatial explosion of the diagnostic model, the concept of the transition influence factor is proposed to replace the traditional transition credibility. At the same time, the parameter setting and adjustment in the traditional fault-diagnosis method are completely dependent on expert experience, and the parameter setting lacks regularity. To reduce the fault-diagnosis error caused by human subjective factors, the comprehensive learning particle swarm optimization algorithm was used to carry out supervised training on the fault-diagnosis model to obtain the system parameter set with self-adaptability. Therefore, the synthetic particle swarm fuzzy Petri Net was defined as a 12-tuple in the equation as follows:

$$S_{CIPSoPRN} = (P, T, I, O, M, W, H, a, B, S, D, K) \quad (1)$$

- (1) $P = \{p_1, p_2, \dots, p_n\}$; P represents the collection of libraries.
- (2) $T = \{t_1, t_2, \dots, t_m\}$; T represents the change set.
- (3) I is the input matrix, representing the mapping of the library to the transition.
- (4) O is the output matrix, representing the mapping of transitions to the library.
- (5) $M = (m_1, m_2, \dots, m_n)$, representing the distribution vector identified by the library.
- (6) $W = (\omega_{ij})$ is the matrix of library weight $n \times m$, representing the influence degree of the input database on the transition.
- (7) $H = (\lambda_1, \lambda_2, \dots, \lambda_m)$, representing the transition threshold distribution vector.
- (8) $a = (a_1, a_2, \dots, a_n)$, $a_i \in [0, 1]$ represents the confidence of the event represented by the p_i of the library.
- (9) $B = (b_1, b_2, \dots, b_r)$; b represents the transition influence factor, representing the ability of the transition to influence its output library, where r represents the number of all arcs from the transition to its output library.
- (10) S represents the number of particles in the comprehensive learning particle swarm optimization algorithm.
- (11) D represents the dimension of the particle in the comprehensive learning particle swarm optimization algorithm.
- (12) K represents the number of iterations.

4.2.1. Structure Optimization

In the traditional fault-diagnosis method based on a Petri net, the fault-diagnosis model is prone to space explosion due to the influence of the system structure. Based on the traditional FPN, the concept of the transition impact factor is proposed in this paper. Through the change in the transition impact factor, the complex logic relationship between each module of the system can be reflected, the expression ability of fault logic between each module of the bearing can be improved, and the space explosion problem of the bearing fault-diagnosis model can be suppressed. Combined with discrete data processing, the bearing fault-diagnosis model shown in Figure 6 was obtained. Figure 6a was the fault-diagnosis model based on the FPN principle, and the blank matrix is the optimized transition. Figure 6b shows that the transition influence factor can play a role in optimizing the model structure, reducing unnecessary transitions, simplifying matrix calculations and helping to suppress the space explosion problem.

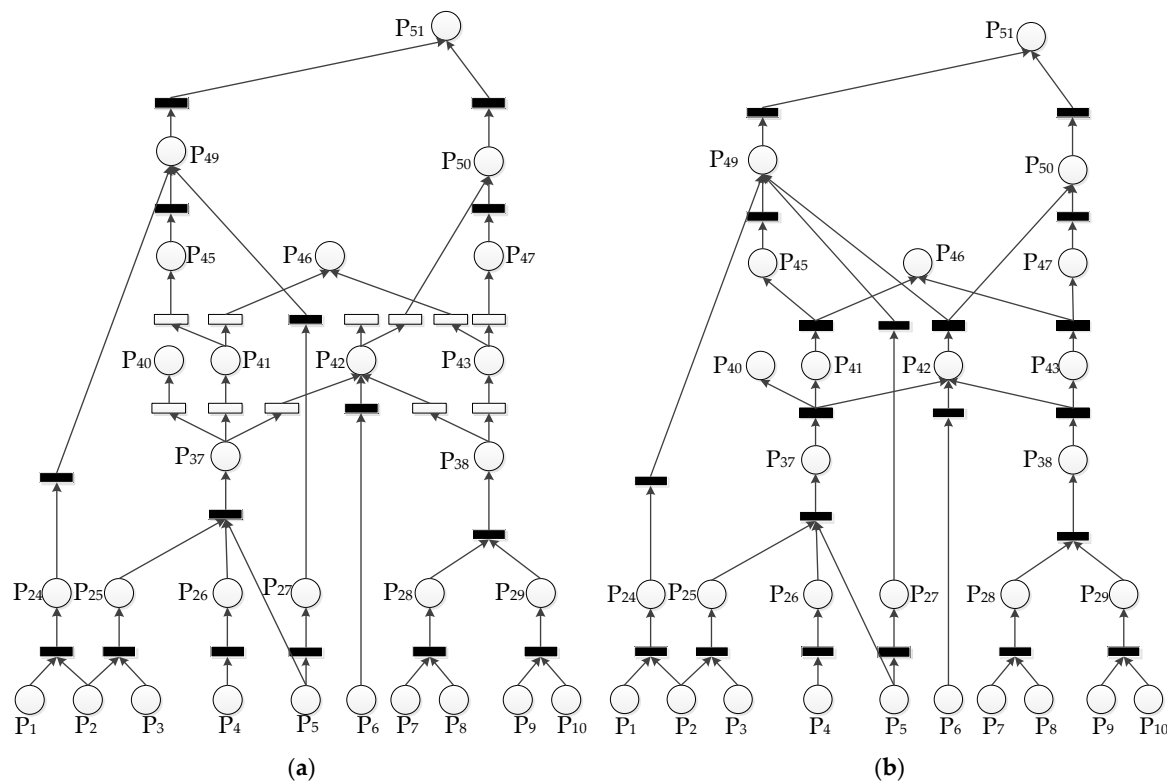


Figure 6. The model of bearing fault. (a) Fault-diagnosis model based on FPN; (b) fault-diagnosis model based on CLPSO-FPN.

4.2.2. Parameter Optimization

PSO is an optimization algorithm established to simulate the foraging behavior of birds in intelligent algorithms. It can realize the function of searching the optimal value by simulating the cooperation and information transmission among individuals in the birds. PSO mainly includes two elements: speed and position. The position of each particle represents a possible solution of the equation, and the velocity represents the direction and step of updating the possible solution. In PSO, the position and velocity of each particle are randomly generated first, and then the individual velocity is updated by judging the global optimal and local optimal position of the population, and the optimization is finally achieved through iteration. However, in a complex system, the nonlinearity and complexity of the logical relationship between modules lead to large differences in the parameters of different dimensions in particles, and unified updating of particles causes the loss of the differences between parameters of different dimensions, resulting in poor local optimization ability.

Based on the limitations of the above PSO, the comprehensive learning particle swarm optimization algorithm is a new intelligent optimization algorithm based on PSO and combined with a comprehensive learning strategy. In contrast to the particle swarm algorithm, which uses particles as the optimization unit, the optimization unit of the comprehensive learning particle swarm optimization algorithm is the different dimensions of particles. As a result, the problem of the parameters of each dimension of the particle being significantly different can be addressed. At the same time, the local optimal target is changed from its own local optimal value to the local optimal value obtained through the comparison of randomly selected particles, which improves the local optimal ability of the algorithm and reduces the fault-diagnosis error caused by human subjective factors. Compared with PSO, it is more suitable for parameter optimization of the complex system fault-diagnosis models. The velocity and position update formulas of the comprehensive learning particle swarm optimization algorithm are shown below.

The CLPSO speed update formula is as follows:

$$V_i^d = k * V_i^d + c_1 * rand1_i^d * (L_p^d - L_i^d) + c_2 * rand2_i^d * (L_g^d - L_i^d) \quad (2)$$

The CLPSO position update formula is as follows:

$$L_i^d = L_i^d + V_i^d \quad (3)$$

where $*$ represents multiplication, k is a real number in the range of inertia constant $[0, 1]$, c is a real number in the range of learning factor $[0, 2]$, $rand$ represents random number, and $rand1_i^d$ and $rand2_i^d$ represent two independent random numbers in the d dimension of the i th particle, whose value is a random number in the range of $[0, 1]$. V_i^d and L_i^d represent the velocity and position of the d dimension parameter of the i th particle, respectively. L_p^d and L_g^d represent particles at locally and globally optimal positions, respectively. The training process is shown in Figure 7.

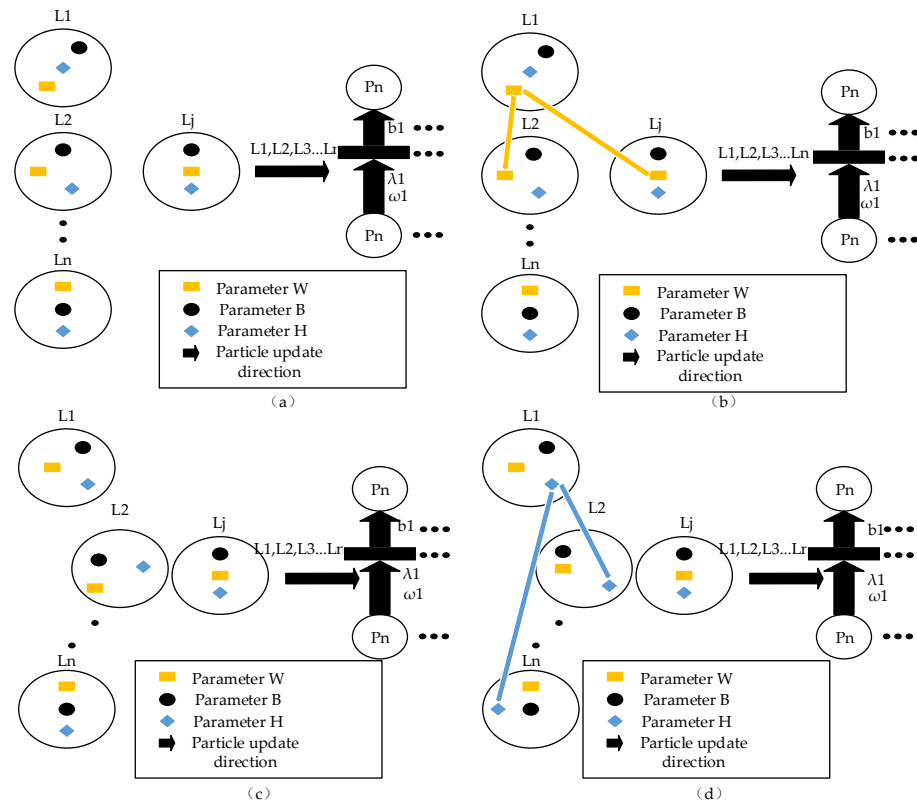


Figure 7. Parameter generation process based on CLPSO.

The parameters of the fault-diagnosis model are trained according to the four fault states in Table 3. Reference [32] defines the particle number $S = 200$, dimension $D = 43$ and the number of iterations $K = 2000$, and the error formula used in the optimization process is as follows:

$$E = \frac{1}{2} * \sum_{i=1}^n (a(p_i) - a^E(p_i))^2 \quad (4)$$

In the formula, $\alpha(p_i)$ and $\alpha^E(p_i)$ represent the confidence of the i th library obtained through confidence reasoning and data statistics, respectively.

The average error under the four operating states is as follows:

$$E = (E_1 + E_2 + E_3 + E_4) / 4 \quad (5)$$

The error value is calculated from the system parameters in the global optimal particles obtained after the training. To ensure the optimality of the training results, the average error of the four kinds of faults are obtained through 400 independent training sessions. The four fault mean error curves shown in Figure 8 are obtained. According to the error curve, the average error is less than 4×10^{-3} . The initial parameter set of the system is selected as the particle value with the minimum average error. When the training is to the 11th iteration, the minimum average error E is as follows: $E = 2.695 \times 10^{-8}$. At this point, the training errors of the four faults are as follows: $E_1 = 4.074 \times 10^{-9}$, $E_2 = 3.6414 \times 10^{-10}$, $E_3 = 5.034 \times 10^{-8}$, $E_4 = 5301 \times 10^{-8}$. It is proven that the integrated particle swarm optimization algorithm has excellent global optimization ability and local optimization ability.

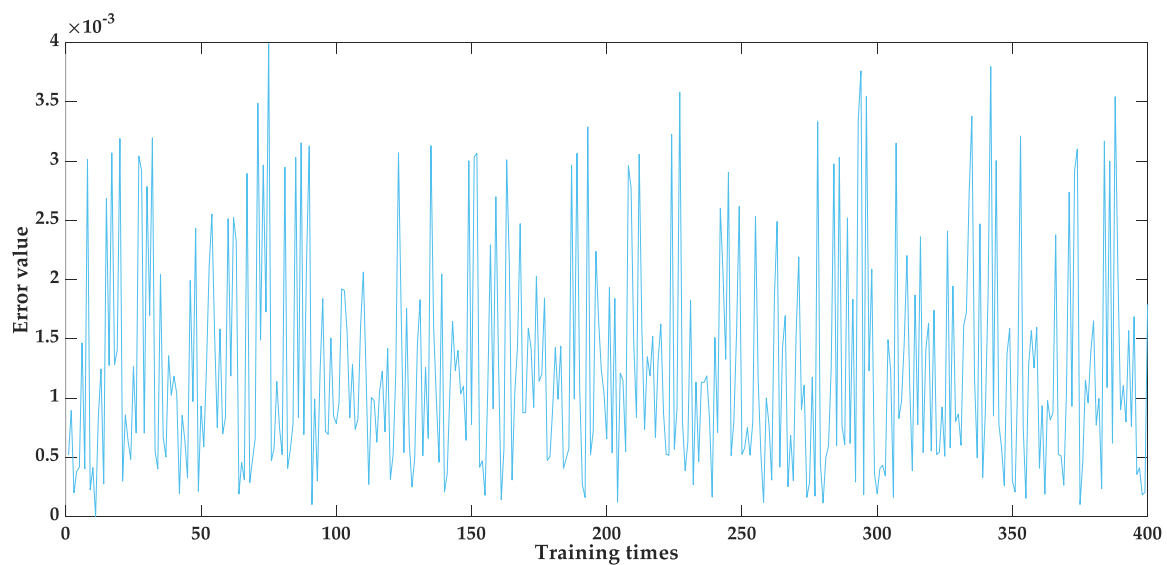


Figure 8. Error curves of E .

4.3. Reasoning Optimization

After the discrete signal processing system is activated, fault reasoning is carried out according to the principle of CLPSO-FPN fault diagnosis, which is specifically divided into two parts: forward reasoning and reverse reasoning. On the premise of locating the bottom fault, forward reasoning realizes the transmission of fault information according to the direction of the directed arc, and predicts the probability of the failure of the top fault module by confidence reasoning. Reverse reasoning occurs according to the direction of the directed arc, and locates the top fault and predicts the fault probability of the bottom module by combining with the minimum cut set incidence rate to realize the function of locating and predicting the fault cause.

Aiming at the problem of the multiple mapping relations between the physical structure and the faults of complex three-phase asynchronous motor equipment, and between the faults of the equipment, according to the CLPSO-FPN operation principle, the competition operator, the maximum operator and the direct multiplication operator were defined. Through the operator characteristics, the ability of the algorithm to deal with the complex relations between different modules in the system was improved, and the matrix reasoning process of the algorithm was optimized. Operators were defined as follows:

1. Competition operator ∇ : $C = \nabla A$; A is $m \times n$ matrix, C is n -dimensional vector, then $c_{ij} = \max(a_{ij})$, where $i = 1, \dots, m, j = 1, 2, \dots, n$.
2. Maximum operator \oplus : $C = A \oplus B$; A, B and C are all $m \times n$ matrices, then $c_{ij} = \max(a_{ij}, b_{ij})$, where $i = 1, 2, \dots, m, j = 1, 2, \dots, n$.
3. Direct multiplication operator: $C = A \otimes b$; A and C are $m \times n$ matrices, B is M -dimensional vector, then $c_{ij} = a_{ij} \times b_i$, where $i = 1, 2, \dots, m, j = 1, 2, \dots, n$.

Specific forward reasoning and reverse reasoning processes were as follows:

(1) Forward reasoning

(1) Transition trigger discrimination

Definition: $X = (x_1, x_2, \dots, x_m)$, X is the m dimensional vector equivalent to the sum of the product of the confidence of the library, and the corresponding weight, X_k , is the value generated in the k th iteration. This can be demonstrated as follows:

$$X_k = (a_k * M_k) \cdot W \quad (6)$$

To improve the reasoning efficiency of the algorithm, a sigmoid function is introduced to determine the transition trigger by matrix calculation as follows:

$$S_k = \frac{1}{A_m + \exp[-d(X_k - H_k)]} \quad (7)$$

where d is positive infinity and $S = (S_1, S_2, \dots, S_m)$ is the trigger vector of the transition, so that when $x > \lambda$, the trigger condition $S_i = 1$ is satisfied. When $x \leq \lambda$, $S_i = 0$, and S_k is the transition triggering vector generated in the k th iteration.

(2) Fault propagation reasoning

The forward reasoning process of CLPSO-FPN reflects the dynamic propagation path of system faults, in which the token reflects the failure situation of each module of the system. With the trigger of change, the token is transferred from the input library to the output library. In a Petri net, the distribution of tokens is called the library identifier, and is represented by vector M . The fault propagation inference formula is as follows:

$$M_{k+1} = M_k \oplus \left[\frac{1}{A_n + \exp[-d((S_k \cdot O^T) - A_n)]} \right] \quad (8)$$

where M_k is the vector identified by the library generated in the k th iteration, and the change of the vector reflects the change of Token in the library. A represents an n -dimensional row vector with elements of 1.

(3) Confidence reasoning

To determine the confidence of the library in the CLPSO-FPN model, based on the traditional fuzzy Petri net, this paper uses the Gaussian function $1 / \exp(10b * (x - 1)^2)$ to replace the transition confidence and uses the transition influence Factor b to reflect the influence ability of the transition on the output database. At the same time, due to the competitive relationship encountered in the fault-diagnosis process of Petri nets, the competitive operator is introduced to optimize the matrix reasoning method, and the optimized confidence reasoning formula is shown as follows:

$$a_{k+1} = a_k \oplus \left[\nabla \left(\left(\frac{X_k}{\exp[10B_k * (X_k - A_m)^2]} \right)^T \otimes O^T \right) \right] \quad (9)$$

where a_k is the confidence vector of the library generated in the k th iteration. According to the requirement of fault-diagnosis reasoning of the CLPSO-FPN algorithm, the reasoning ends when $a_{k+1} = a_k$.

(2) Reverse reasoning

(1) Transition trigger discrimination

The way to determine the transition trigger of reverse reasoning is different from that of forward reasoning. The transition trigger does not need to meet the condition of the transition threshold, and information transfer from the transition output database to the

input database is inevitable. Therefore, the reverse transition trigger formula is defined as follows:

$$S_k^- = M_k^- \cdot I^- \quad (10)$$

where S_k^- is the reverse transition triggering vector generated in the k th iteration and $I^- = O$ is the input matrix of reverse reasoning, namely, the output matrix of forward reasoning.

(2) Fault propagation reasoning

The fault propagation reasoning of reverse reasoning is different from that of forward reasoning. Forward fault propagation reasoning reflects the dynamic propagation path of the system fault. Reverse reasoning reflects the bottom fault related to the top fault, that is, the various causes of the fault. To improve the matrix reasoning ability of the algorithm, the backward fault propagation reasoning formula is defined as follows:

$$M_{k+1}^- = M_k^- \oplus \left[\frac{1}{A_n + \exp[-b((S_k^- \cdot O^{-T}) - A_n)]} \right] \quad (11)$$

where M_k^- is the vector identified by the reverse library generated in the k th iteration, and $O^- = I$ is the output matrix of reverse reasoning, namely, the input matrix of forward reasoning. When $M_{k+1}^- = M_k^-$, the reasoning ends.

(3) Confidence reasoning

Since both transition triggers and fault propagation are inevitable in the reverse reasoning process, the probability of each module's fault occurrence cannot be obtained by using the forward confidence reasoning method. To address the problem of the confidence value being unobtainable by backward reasoning, the minimum cut set sorting method was introduced. When the top-level module fails, the bottom fault that causes the top fault can be obtained through reverse transition trigger and fault propagation reasoning. Finally, the probability of occurrence of each bottom fault module can be obtained through the sorting method of the minimum cut set to avoid overhaul blindness, improve the efficiency of bearing fault troubleshooting and maintenance and be conducive to the stability of system operation. If the minimum cut set is $G = \{p_1, p_2, \dots, p_n\}$, the probability formula of the occurrence of the minimum cut set is shown as follows:

$$G = \frac{p_1 + p_2 + \dots + p_n}{n} \quad (12)$$

5. Experiments and Discussion

The sampling frequency of the data was 12 kHz. The data were composed as follows: sampling points 1 to 1200 were bearing data in normal state, sampling points 1201 to 2400 were data in case of rolling element failure, sampling points 2401 to 3600 were data in case of inner ring failure, and sampling points 3601 to 4800 were data in case of outer ring failure. In order to verify the effectiveness of the fault-diagnosis method in this paper, the fault tree method was introduced to carry out fault reasoning for motor-bearing faults, and the effectiveness of the method was verified by comparing the diagnosis results. "Rolling element failure", "inner race failure" and "outer race failure" were taken as examples for verification and comparison, and the bearing fault tree was established, as shown in Figure 9.

The competition relationship in Petri nets is represented by the OR logic consisting of X_{15} and X_{19} . In this case, if two events occurred at the same time, the event with the largest probability value would be selected as the trigger condition of X_{20} . According to the trigger rule calculation, the probability value $X_{20} = 0.790$ of X_{20} was derived, and the calculation result was consistent with that of CLPSO-FPN, which proved the effectiveness of the fault-diagnosis method in this paper.

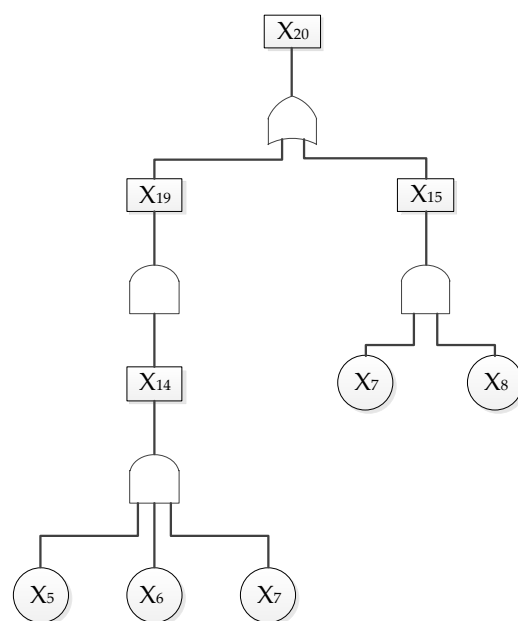


Figure 9. Bearing fault tree analysis.

Due to the influence of fuzzy theory, the system parameters of fuzzy Petri nets are often assigned by expert experience, and the accuracy of fault diagnosis is low, which makes it difficult to meet the needs of fault diagnosis of complex systems. In order to solve the above problems, a fuzzy Petri net fault-diagnosis method based on the artificial intelligence algorithm was proposed. Based on the strong self-learning and optimization ability of the artificial intelligence algorithm, the fuzzy and empirical problems of the system parameters were effectively solved, and the accuracy of the system fault diagnosis was improved. At present, BP neural network and particle swarm optimization algorithms are often used in the optimization algorithm of fuzzy Petri nets. In order to verify the optimization ability of the integrated particle swarm optimization algorithm proposed in this paper for fault diagnosis of fuzzy Petri nets, CLPSO algorithm, PSO algorithm and BP neural network algorithm were used to optimize the fault-diagnosis model of three-phase asynchronous motors. Through the forward reasoning analysis of the three fault states, the accuracy of fault diagnosis of FPN, BP-FPN, PSO-FPN and CLPSO-FPN was compared.

For FPN-based fault diagnosis, the parameters of weight W , threshold h and transition influence factor B were obtained by expert experience, where threshold $\lambda = 0.2$, and $b = 0.3$. For fault diagnosis based on BP-FPN, the initial parameters of its weight W , threshold h and transition influence factor B were the same as those of FPN, and the number of iterations was $k = 1000$. The fault-diagnosis process based on PSO-FPN was similar to the fault-diagnosis process based on CLPSO-FPN, with $k = 400$ iterations and $S = 200$ particles.

According to the analysis in Section 4.2, the initial parameter set of the system was selected as the particle value for the minimum average error, and the weight value (as shown in Table 4), threshold value and transition impact factor of the fault-diagnosis model obtained at this time were as follows.

Table 4. The optimized weight table by CLPSO.

Parameter	Weight	Parameter	Weight	Parameter	Weight
$\omega_{1,1}$	0.5237	$\omega_{2,1}$	0.4763	$\omega_{3,2}$	0.2457
$\omega_{4,2}$	0.7543	$\omega_{5,3}$	0.2146	$\omega_{6,3}$	0.2577
$\omega_{7,3}$	0.5277	$\omega_{7,4}$	0.6497	$\omega_{8,4}$	0.3503
$\omega_{9,5}$	0.6175	$\omega_{10,5}$	0.3825	$\omega_{12,7}$	0.3397
$\omega_{13,7}$	0.6603	$\omega_{18,11}$	0.2083	$\omega_{14,11}$	0.7917

The remaining weights were set as 1, according to the fuzzy Petri net theory.

$H = (0.2689, 0.3174, 0.5972, 0.1839, 0.8000, 0.1619, 0.6541, 0.4163, 0.2243, 0.5121, 0.0821, 0.1101)$.

$B = (0.0254, 0.2060, 0, 0.1358, 0.4891, 0.1715, 0.0883, 0.0585, 0, 0.1016, 0, 0, 0)$.

The comparison of the diagnosis results and the algorithm are shown in Table 5. Table 5 shows that compared with the fuzzy Petri net fault-diagnosis method, the fault-diagnosis method optimized by the artificial intelligence algorithm had considerably improved fault-diagnosis accuracy. Among them, BP-FPN had excellent local optimization ability but poor global optimization ability, which easily demonstrated the missing judgement phenomenon. The PSO-FPN method has a strong global optimization capability, but it has the problem of insufficient local optimization capability for complex system fault diagnosis. Compared with the other three fault-diagnosis methods, the CLPSO-FPN method proposed in this paper has excellent global and local optimization capabilities, which can accurately predict bearings, prevent the failure of fault diagnosis and meet the requirements of fault-diagnosis accuracy for complex motor systems.

Table 5. The table of fault-diagnosis results. (a) The table of fault causes and diagnosis results; (b) the table of failure probability and accuracy.

(a)				
Diagnosis Way	Cause of the Problem	Results of Diagnosis	Terminal Malfunction	
FPN	p_6, p_7, p_8 p_9, p_{10}, p_{11}	p_{14}, p_{15}, p_{20} $p_{16}, p_{17}, p_{20}, p_{17}$	p_{20}	
			p_{20}	
			p_{20}	
			p_{20}	
BP-FPN	p_6, p_7, p_8 p_9, p_{10}, p_{11}	p_{15}, p_{20}, p_{16} $p_{17}, p_{20}, \text{nothing}$	p_{20}	
			p_{20}	
			p_{20}	
			p_{20}	
PSO-FPN	p_6, p_7, p_8 p_9, p_{10}, p_{11}	p_{14}, p_{15}, p_{20} $p_{16}, p_{17}, p_{20}, p_{17}$	p_{20}	
			p_{20}	
			p_{20}	
			p_{20}	
CLPSO-FPN	p_6, p_7, p_8 p_9, p_{10}, p_{11}	$p_{14}, p_{15}, p_{19}, p_{20}$ $p_{16}, p_{17}, p_{20}, p_{17}, p_{20}$	p_{20}	
			p_{20}	
			p_{20}	
			p_{20}	
(b)				
Diagnosis Way	Actual Failure Probability	Diagnostic Fault Probability	Accuracy	Computation Time
FPN	0.790	0.611	77.4%	1.5924S
	0.769	0.536	69.7%	
	0.590	0.182	30.9%	
	0.790	0.790	100%	
BP-FPN	0.769	0.601	78.2%	1.7049S
	0.590	0	0	
	0.790	0.771	97.6%	
	0.769	0.625	81.3%	
PSO-FPN	0.590	0.6075	97.0%	1.7918S
	0.790	0.790	100%	
	0.769	0.768	99.9%	
	0.590	0.583	98.8%	

6. Conclusions

Aiming at the problems of the traditional Petri net fault-diagnosis method with a single input signal and the lack of integrity and timeliness of the traditional motor-bearing fault-diagnosis method, a motor-bearing fault-diagnosis method based on CLPSO-FPN was proposed, and the following conclusions were drawn:

- (1) The EMD method is used to effectively process the acquired fault signals, and discrete fault classification signals are obtained to activate the discrete signal processing system. This addresses the problem that occurs when the traditional quantitative analysis method lacks integrity in fault diagnosis and the qualitative analysis method lacks timeliness in fault diagnosis.
- (2) The concept of the transition influence factor is defined, the structure of the fault-diagnosis model is optimized and the space explosion of the fault-diagnosis model of a complex system is restrained. A comprehensive learning particle swarm optimized fuzzy Petri net algorithm is proposed to optimize the parameters of the fault-diagnosis model, improve the adaptability of the fault-diagnosis model, reduce the influence of human subjective factors on the fault-diagnosis results and improve the accuracy of fault identification.

Author Contributions: Conceptualization, C.X.; data curation, C.X.; formal analysis, C.X.; funding acquisition, X.C.; investigation, J.L.; methodology, C.X.; project administration, X.C.; resources, X.C.; software, C.X. and J.L.; supervision, X.C. and J.L.; validation, C.X. and J.L.; writing—original draft, C.X.; writing—review and editing, C.X. All authors have read and agreed to the published version of the manuscript.

Funding: This research was funded by the National Natural Science Foundation of China Program (No. 62073198), the Major Research Development Program of Shandong Province of China (No. 2016GSF117009).

Institutional Review Board Statement: Not applicable.

Informed Consent Statement: Not applicable.

Data Availability Statement: Not applicable.

Acknowledgments: The Project (work) was supported by the National Natural Science Foundation of China Program (No. 62073198) and the Major Research Development Program of Shandong Province of China (No. 2016GSF117009).

Conflicts of Interest: The authors declare no conflict of interest.

Abbreviations

CLPSO-FPN	comprehensive learning particle swarm optimized fuzzy Petri net
EMD	empirical mode decomposition
PCA	principal component analysis
SVM	support vector machine
PSO	particle swarm optimization
IMFs	intrinsic mode functions
TSHFPNs	time sequence hierarchical fuzzy Petri nets

References

1. Hou, H.; Ji, H.Q. Improved multiclass support vector data description for planetary gearbox fault diagnosis. *Control Eng. Pract.* **2021**, *114*, 104867. [\[CrossRef\]](#)
2. Choudhary, A.; Goyal, D.; Shimi, S.L.; Akula, A. Condition Monitoring and Fault Diagnosis of Induction Motors: A Review. *Arch. Comput. Methods Eng.* **2019**, *26*, 1221–1238. [\[CrossRef\]](#)
3. Gangsar, P.; Tiwari, R. Signal based condition monitoring techniques for fault detection and diagnosis of induction motors: A state-of-the-art review. *Mech. Syst. Signal Process.* **2020**, *144*, 106908. [\[CrossRef\]](#)
4. Zhang, G.W.; Han, B.K.; Li, S.M.; Wang, J.R. General normalized maximum mean discrepancy: Intelligent fault identification method for bearings and gears under unstable conditions. *Meas. Sci. Technol.* **2021**, *32*, 104001. [\[CrossRef\]](#)
5. Sim, K.; Lee, Y.B.; Jang, S.M.; Kim, T.H. Thermal analysis of high-speed permanent magnet motor with cooling flows supported on gas foil bearings: Part II—Bearing modeling and case studies. *J. Mech. Sci. Technol.* **2015**, *29*, 5477–5483. [\[CrossRef\]](#)
6. Yang, J.H.; Wu, C.J.; Shan, Z.; Liu, H.G. Extraction and enhancement of unknown bearing fault feature in the strong noise under variable speed condition. *Meas. Sci. Technol.* **2021**, *32*, 105021. [\[CrossRef\]](#)
7. Galezia, A.; Gryllias, K. Application of the Combined Teager-Kaiser Envelope for bearing fault diagnosis. *Measurement* **2021**, *182*, 109710. [\[CrossRef\]](#)

8. Deng, W.; Zhang, S.J.; Zhao, H.M.; Yang, X.H. A Novel Fault Diagnosis Method Based on Integrating Empirical Wavelet Transform and Fuzzy Entropy for Motor Bearing. *IEEE Access* **2018**, *6*, 35042–35056. [\[CrossRef\]](#)
9. Xu, K.; Chen, Z.H.; Zhang, C.B.; Dong, G.Z. Rolling bearing fault diagnosis based on empirical mode decomposition and support vector machine. *Control Theory Appl.* **2019**, *36*, 915–922.
10. Li, Y.; Zhang, W.; Xiong, Q.; Luo, D.; Tao, Z. A rolling bearing fault diagnosis strategy based on improved multiscale permutation entropy and least squares SVM. *J. Mech. Sci. Technol.* **2017**, *31*, 2711–2722. [\[CrossRef\]](#)
11. Xiao, X.; Xiao, Y.X.; Zhang, Y.J. Research on the Application of the Data Augmentation Method Based on 2D Gray Pixel Images in the Fault Diagnosis of Motor Bearing. *Proc. CSEE* **2021**, *41*, 738–749.
12. Zhu, G.; Feng, L.; Li, Z.; Wu, N. An Efficient Fault Diagnosis Approach Based on Integer Linear Programming for Labeled Petri Nets. *IEEE Trans. Autom. Control* **2021**, *66*, 2393–2398. [\[CrossRef\]](#)
13. Zhang, Y.; Zhang, Y.; Wen, F.; Chi, Y.C. A fuzzy Petri Net based approach for fault diagnosis in power systems considering temporal constraints. *Int. J. Electr. Power Energy Syst.* **2016**, *78*, 215–224. [\[CrossRef\]](#)
14. Arichi, F.; Cherki, B.; Djemai, M.; Djouadi, S.M. Fault diagnosis for discrete events systems described by partially observed Petri nets. *ISA Trans.* **2021**, *128*, 220–228. [\[CrossRef\]](#)
15. Yue, W.C.; Gui, W.H.; Chen, X.F.; Zeng, Z.H.; Xie, Y.F. Knowledge representation and reasoning using self-learning interval type-2 fuzzy Petri Nets and extended TOPSIS. *Int. J. Mach. Learn. Cybern.* **2019**, *10*, 3499–3520. [\[CrossRef\]](#)
16. David, R.; Alla, H. Petri nets for modeling of dynamic systems: A survey. *Nat. Comput.* **2010**, *9*, 955–989. [\[CrossRef\]](#)
17. Zhong, C.F.; He, W.L.; Li, Z.W.; Wu, N.Q. Deadlock Analysis and Control Using Petri Net Decomposition Techniques. *Inf. Sci.* **2019**, *482*, 440–456. [\[CrossRef\]](#)
18. Chen, C.; Yang, Y.B.; Wang, M.T.; Zhang, X. Characterization and evolution of emergency scenarios using hybrid Petri net. *Process Saf. Environ. Prot.* **2018**, *114*, 33–142. [\[CrossRef\]](#)
19. Fazzinga, B.; Folino, F.; Furfaro, F.; Pontieri, L. An ensemblebased approach to the security-oriented classification of low-level log traces. *Expert Syst. Appl.* **2020**, *153*, 113386. [\[CrossRef\]](#)
20. Bustos, A.; Rubio, H.; Castejon, C.; Garcia-Prada, J.C. EMD-Based Methodology for the Identification of a High-Speed Train Running in a Gear Operating State. *Sensors* **2018**, *18*, 793. [\[CrossRef\]](#)
21. Bustos, A.; Rubio, H.; Castejon, C.; Garcia-Prada, J.C. Condition monitoring of critical mechanical elements through Graphical Representation of State Configurations and Chromogram of Bands of Frequency. *Measurement* **2019**, *135*, 71–82. [\[CrossRef\]](#)
22. Al-Ajeli, A.; Parker, D. Fault diagnosis in labelled Petri nets: A Fourier–Motzkin based approach. *Automatica* **2021**, *132*, 109831. [\[CrossRef\]](#)
23. Smith, W.A.; Randall, R.B. Rolling element bearing diagnostics using the Case Western Reserve University data: A benchmark study. *Mech. Syst. Signal Process.* **2015**, *64–65*, 100–121. [\[CrossRef\]](#)
24. Zhao, L.; Wang, J.; Zhang, W.C. Smooth Adaptive Internal Model Control Based on U Model for Nonlinear Systems with Dynamic Uncertainties. *Math. Probl. Eng.* **2016**, *2016*, 2926914. [\[CrossRef\]](#)
25. Xu, Z.; Tang, G.; He, M.F. Peak-Based Mode Decomposition for Weak Fault Feature Enhancement and Detection of Rolling Element Bearing. *Shock Vib.* **2020**, *2020*, 8901794. [\[CrossRef\]](#)
26. Li, Y.; Zhu, Q.M.; Zhang, J.H. Distributed adaptive fixedtime neural networks control for nonaffine nonlinear multiagent systems. *Sci. Rep.* **2022**, *12*, 8459. [\[CrossRef\]](#)
27. Kang, S.Q.; Wang, Y.J.; Yang, G.X.; Song, L. Rolling Bearing Fault Diagnosis Method Using Empirical Mode Decomposition and Hypersphere Multiclass Support Vector Machine. *Proc. CSEE* **2011**, *31*, 96–102.
28. Peng, Y.W.; Ma, X.H. A Fault Diagnosis Method of Rolling Bearings Based on Parameter Optimization and Adaptive Generalized S-Transform. *Machines* **2022**, *10*, 207. [\[CrossRef\]](#)
29. Bhavsar, K.; Vakharia, V.; Chaudhari, R.; Vora, J.; Pimenov, D.Y.; Giasin, K. A Comparative Study to Predict Bearing Degradation Using Discrete Wavelet Transform (DWT), Tabular Generative Adversarial Networks (TGAN) and Machine Learning Models. *Machines* **2022**, *10*, 176. [\[CrossRef\]](#)
30. Li, J.M.; Zhu, X.L.; Cheng, X.Z. Sensor fault diagnosis based on fuzzy neural Petri net. *Complexity* **2018**, *2018*, 8261549. [\[CrossRef\]](#)
31. Kabir, S.; Papadopoulos, Y. Applications of Bayesian networks and Petri nets in safety, reliability, and risk assessments: A review. *Saf. Sci.* **2019**, *115*, 154–175. [\[CrossRef\]](#)
32. Cheng, X.Z.; Wang, C.A.; Li, J.M. Adaptive fault diagnosis of motors using comprehensive learning particle swarm optimizer with fuzzy petri net. *Comput. Inform.* **2020**, *39*, 246–263. [\[CrossRef\]](#)